

# Comparison of Different off Bottom Impeller Clearances to Investigate the Effect on Hydrodynamics in Rushton Turbine Stirred Tank

Harshal Patil<sup>1</sup>, Ajey Kumar Patel<sup>2\*</sup>, K. Devarajan<sup>2</sup>, A. Venu Vinod<sup>1</sup>

<sup>1</sup>Department of Chemical Engineering, National Institute of Technology Warangal, Warangal-506004

<sup>2</sup>Department of Civil Engineering, National Institute of Technology Warangal, Warangal-506004

\*Corresponding author: ajeypatel@gmail.com

## ABSTRACT

Flow fields and turbulence quantities are important considerations in the design of stirred tanks for many industrial processes. A series of Computational Fluid Dynamics (CFD) simulations have been conducted in present work to investigate the flow hydrodynamics of fully baffled Rushton turbine stirred tank at various impeller clearances ranging from  $C/T = 0.33$  to  $C/T = 0.15$ . It is well known that double circulation loop flow pattern changes to single circulation loop flow pattern at lower impeller clearances in baffled stirred tanks. But the exact clearance at which flow pattern transition occurs is not clearly known. Thus the main objective of the present study is to determine exact location of flow pattern transition as well as to analyse the changes in flow hydrodynamics with impeller clearance. The double to single loop transition occurs exactly at  $C^* = C/T = 0.18$  and sharp decrease in power number and pumping number were obtained. Further, power number, pumping number and radial velocity fields decreased, while axial velocity fields increased below the impeller centre plane beyond the  $C^*$ . The turbulent kinetic energy also reduced as the impeller clearances reduced. Thus radial as well as turbulent action of Rushton turbine changes to axial nature as impeller clearance reduces below  $C^*$ .

**Keywords:** Rushton Turbine, stirred tanks, CFD, impeller clearance, power consumption, mixing, MRF.

## 1 INTRODUCTION

Stirred tanks with Rushton turbine impeller are widely adopted for mixing operations in various chemical as well as allied industries. Efficient design of stirred tank is quite important to achieve necessary flow conditions at minimum energy requirements. Energy optimized design of stirred tanks can be obtained by proper adjustment of its geometric parameters. It is well known that, the off bottom impeller clearance is one of the crucial parameters which significantly affects the power consumption, pumping capacity and degree of mixing in stirred tanks [1,2]. In this view, various numerical and experimental investigations [3-6] decreased the off bottom impeller clearance to provide required axial mixing for solid suspension operation at lesser power consumption. But the exact impeller clearance at which flow hydrodynamics as well as power number drastically changes is not clearly identified. Thus the main objective of the present study is to determine exact location and to analyse the changes in flow hydrodynamics with impeller clearance. This study uses the CFD technique to accomplish the objective due to various limitations associated with experimental studies.

## 2 STIRRED VESSEL CONFIGURATION

The simulations have been performed for standard cylindrical stirred tank. It was employed with four equally spaced baffles and six bladed Rushton turbine. The tank diameter ( $T$ ) was kept to 30 cm and filled with water level ( $H$ ) equal to tank diameter. The thickness of blade and turbine disc was taken to 0.2 cm. The configuration and related dimensions of stirred tank considered are shown in Figure 1. The rotational speed of impeller ( $N$ ) was kept at 200 rpm for Reynolds number of 33173 in the fully turbulent regime. A cylindrical coordinate

system was adopted, with  $r$ ,  $z$  and  $\theta$  indicates the radial, axial and tangential coordinates respectively. Its origin was fixed at centre of impeller hub with  $r$ ,  $z$  and  $\theta = 0^\circ$ .  $V_r$ ,  $V_z$  and  $V_{tip} = \pi ND$  represents the mean radial, mean axial and impeller tip velocity respectively while  $k$  represents the Turbulent Kinetic Energy (TKE).

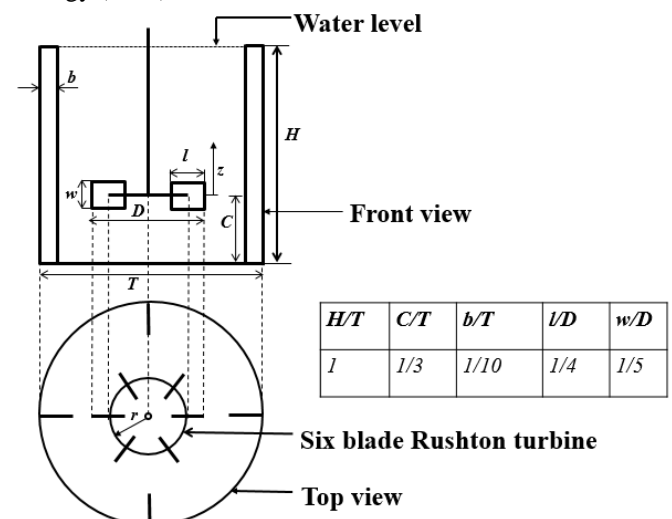


Figure 1: Configuration of Rushton turbine stirred tank

## 3 COMPUTATIONAL METHODOLOGY

CFD simulations have been conducted for various off bottom clearances ranging from  $C/T = 0.33$  (standard configuration) to 0.15. Commercial software package Ansys 17.2 was used for modelling of stirred tank. The flow domain was divided into small volumes and meshing was created using tool

available in Ansys. The mesh was refined close to the impeller swept region as the velocity gradients are very sharp in this region. The mesh sensitivity test was performed at standard clearance ( $C/T = 0.33$ ) to avoid numerical errors (details are addressed in the following section).

Reynolds Averaged Navier-Stokes (RANS) equations coupled with standard  $k - \varepsilon$  turbulence model were used for solution of the flow variables. Multiple Reference Frame (MRF) technique was adopted for impeller rotation model. This technique is more suitable for steady state simulations and gives similar results with less computational expense compared to other techniques. Momentum and turbulence quantities were discretized by second order upwind scheme. The velocity and pressure were coupled through the Semi Implicit Method for Pressure Linked Equations (SIMPLE) algorithm. To attain better convergence and stability in the solution, the under relaxation factor was kept at lower value. The convergence criteria was kept at  $10^{-6}$  for continuity, velocity and turbulence quantities. A no slip boundary condition was adopted for solid surfaces. Standard wall function was used to link the viscosity dominated region between the walls and the fully turbulent region [7].

### 3.1 Model Equations

Flow behavior inside stirred tank was solved by discretized governing equations (Reynolds Averaged Navier Stokes), which solves the mass and momentum conservation equations and provide solution for flow variables such as velocity and pressure. The continuity or mass conservation equation is given by

$$\frac{\partial u}{\partial x} + \frac{\partial v}{\partial y} + \frac{\partial w}{\partial z} = 0 \quad (1)$$

The momentum conservation equations for incompressible flow are given by

$$\rho \frac{Du}{Dt} = \rho g_x - \frac{\partial p}{\partial x} + \mu \left( \frac{\partial^2 u}{\partial x^2} + \frac{\partial^2 u}{\partial y^2} + \frac{\partial^2 u}{\partial z^2} \right) \quad (2)$$

$$\rho \frac{Dv}{Dt} = \rho g_y - \frac{\partial p}{\partial y} + \mu \left( \frac{\partial^2 v}{\partial x^2} + \frac{\partial^2 v}{\partial y^2} + \frac{\partial^2 v}{\partial z^2} \right) \quad (3)$$

$$\rho \frac{Dw}{Dt} = \rho g_z - \frac{\partial p}{\partial z} + \mu \left( \frac{\partial^2 w}{\partial x^2} + \frac{\partial^2 w}{\partial y^2} + \frac{\partial^2 w}{\partial z^2} \right) \quad (4)$$

Where  $u, v$  and  $w$  are the fluid velocities in the  $x, y$  and  $z$  directions respectively and  $p$  is the local pressure.

### 3.2 Turbulence Model

In above RANS equations turbulence was added by decomposing the instantaneous form of flow variables into mean and fluctuating components. Substituting the decomposed form of flow variables into the continuity and momentum equation and taking a time average, yielded the ensemble averaged continuity and momentum equations. The standard  $k - \varepsilon$  is two equation turbulence model which determines the both turbulent length and time scale by solving two separate transport equations for  $k$  and  $\varepsilon$ . After all the modified equations can be written as

$$\frac{\partial}{\partial t}(\rho k) + \frac{\partial}{\partial x_i}(\rho k u_i) = \frac{\partial}{\partial x_j} \left[ \left( \mu + \frac{\mu_t}{\sigma_k} \right) \frac{\partial k}{\partial x_j} \right] + G_k + G_b - \rho \varepsilon - Y_M + S_k \quad (5)$$

and

$$\frac{\partial}{\partial t}(\rho \varepsilon) + \frac{\partial}{\partial x_i}(\rho \varepsilon u_i) = \frac{\partial}{\partial x_j} \left[ \left( \mu + \frac{\mu_t}{\sigma_\varepsilon} \right) \frac{\partial \varepsilon}{\partial x_j} \right] + C_{1\varepsilon} \frac{\varepsilon}{k} (G_k + C_{3\varepsilon} G_b) - C_{2\varepsilon} \rho \frac{\varepsilon^2}{k} + S_\varepsilon \quad (6)$$

In above equations,  $G_k$  and  $G_b$  represents the generation of turbulence kinetic energy due to mean velocity gradients and due to buoyancy respectively.  $Y_M$  represents the contribution of the fluctuating dilatation in compressible turbulence to the overall dissipation rate.  $C_{1\varepsilon}$ ,  $C_{2\varepsilon}$  and  $C_{3\varepsilon}$  are constants.  $\sigma_k$  and  $\sigma_\varepsilon$  are turbulent Prandtl number for  $k$  and  $\varepsilon$  respectively.  $S_k$  and  $S_\varepsilon$  are user-defined source terms [8].

## 4 RESULTS AND DISCUSSIONS

### 4.1 Effect on Power number with variation in impeller clearance

Power number ( $N_p$ ) is one of the important consideration in design of stirred tanks as it directly reflects the power required for stirring.  $N_p$  predicted by simulations have been computed from the torque exerted by stirrer on fluid. To improve the CFD model predictions, series of simulations have been performed at different grid sizes to find the optimal grid size. The effect of grid size on prediction of  $N_p$  at standard clearance is plotted in Figure 2. Improvement in  $N_p$  is observed with increase in number of elements. But for last three grid sizes, no significant improvement is observed. Hence grid size having 2492445 number of elements considered to be optimal size to minimize the computational expenses and same optimal grid size was considered for further impeller clearance simulations.

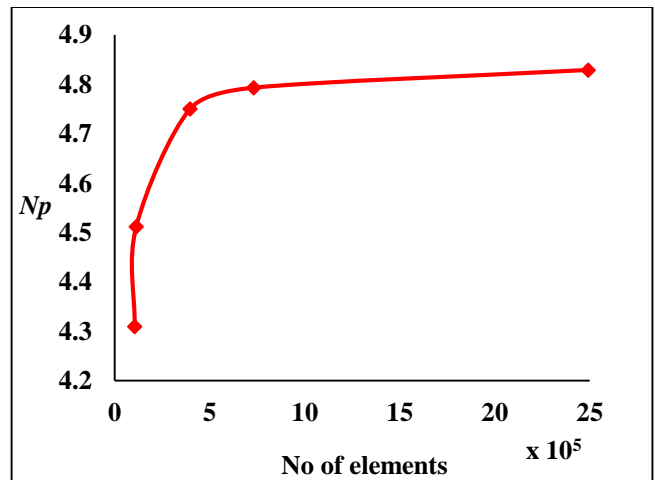


Figure 2: Effect of grid size on Power number

Figure 3 shows the plot for effect on  $N_p$  with variation in impeller clearance. At  $C/T = 0.33$  (standard), the value of  $N_p$  is found to be 4.82 which is expected for standard configuration. The value of  $N_p$  slightly lowers with decreasing the impeller clearance up to  $C/T = 0.19$ . At  $C/T = C^* = 0.18$ , it

suddenly drops to 3.36 and becomes constant for further reduced clearances. The value of  $N_p$  at  $C^*$  was found to be decreased by 30 % relatively in comparison with  $C/T = 0.33$ . Such reduction in power number is useful in solid suspension operation where solids can be lift with lesser power consumption.

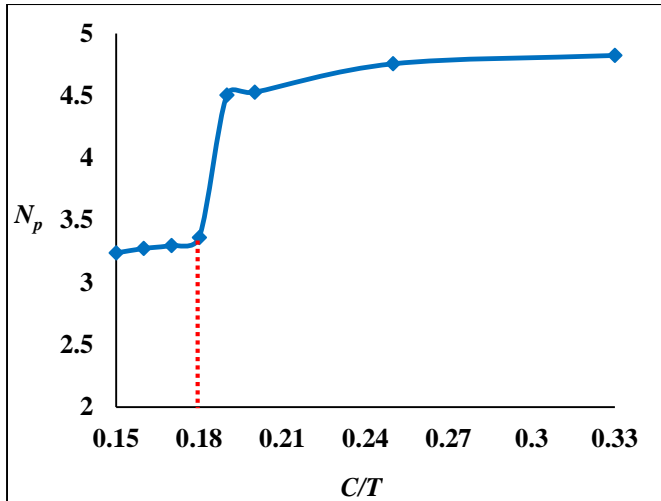
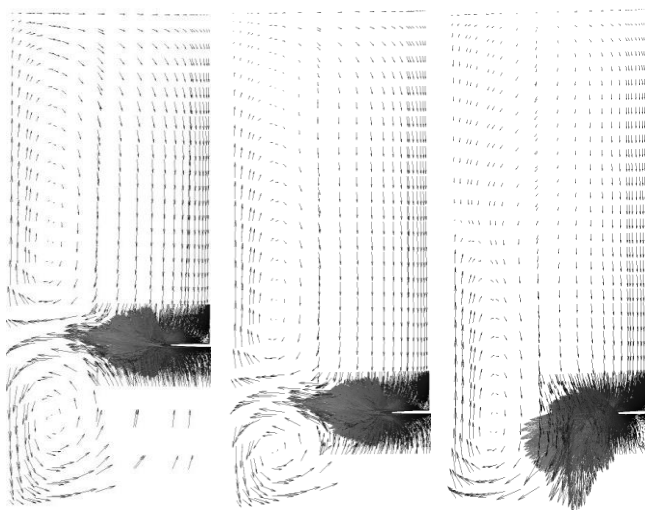


Figure 3: Effect on Power number with variation in impeller clearance

#### 4.2 Double to single circulation loop transition

As explained earlier a series of CFD simulations have been conducted in the context to find the exact the exact clearance of flow transition. The double to single circulation loop flow transition was observed at  $C^*$  where sudden drops in  $N_p$  was found. The comparison of velocity vector plots in  $r$ - $z$  plane at three impeller clearances i.e.  $C/T = 0.33$ , 0.19 and 0.18 is shown in Figure 4. Similar kind of vector plots were observed for remaining clearances, but not presented for economy of presentation. Particularly at  $C^*$  the impeller discharge stream is observed to be inclined towards the bottom of the tank good match with literature data [6].



$C/T = 0.33$  (a)  $C/T = 0.19$  (b)  $C/T = 0.18$  (c)

Figure 4: Velocity vector plots in  $r$ - $z$  plane at  $45^\circ$

#### 4.3 Effect of impeller clearance on mean flow fields

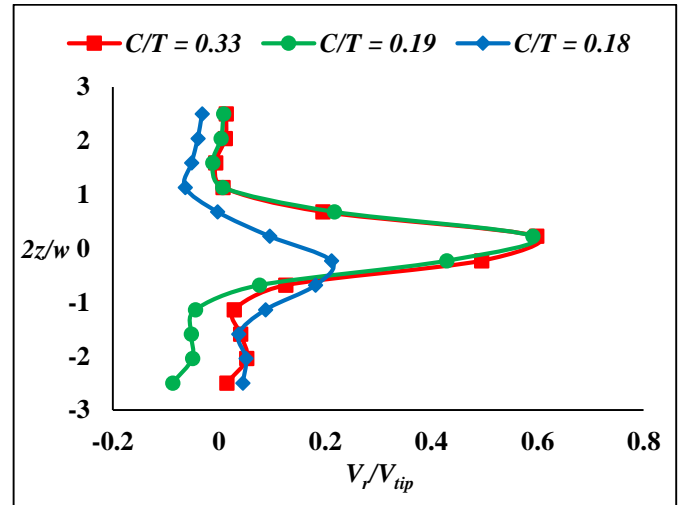


Figure 5: Axial profiles of normalized radial velocity at  $r = 5.55$  cm and  $\theta = 45^\circ$

The knowledge of local flow fields and turbulence quantities is paramount importance in design of stirred tanks. So far considerable focus was intended towards global flow variables to investigate the impeller clearance effect. However the local flow fields and turbulences quantise need to be studied. Figures 5 and 6 show the effect on the axial profiles of normalized radial and axial velocities with variation in impeller clearance. Significant reduction in the peak radial velocity is observed at  $C^*$  compared to other clearances. Interestingly at  $C^*$ , peak of radial velocity is shifted just below the impeller centre plane and inclined downwards. In case of axial velocities, the peak as well as velocity increases below the impeller centre plane at  $C^*$  in comparison with other clearances. Thus the mean flow fields clearly indicates, the nature of flow transformed radial to axial.

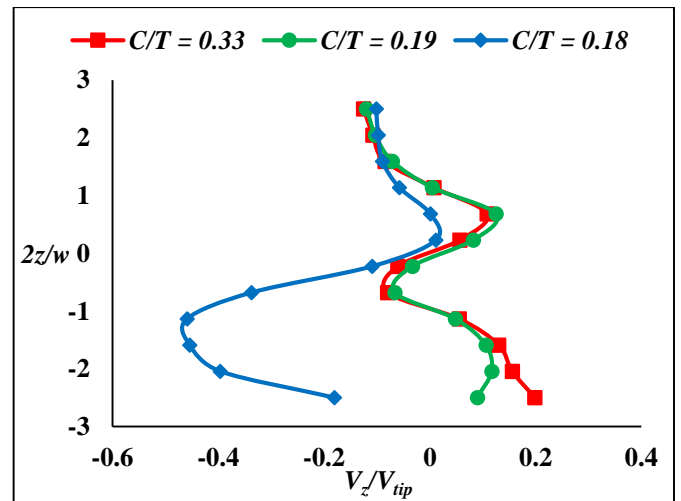


Figure 6: Axial profiles of normalized axial velocity at  $r = 5.55$  cm and  $\theta = 45^\circ$

#### 4.4 Dependency of Radial Pumping number on impeller clearance

Rushton turbine is the radial flow impeller for which effect of impeller clearance on radial pumping capacity needs to be investigated. Here radial pumping capacity is represented in

terms of dimensionless radial pumping number ( $Nr$ ) which represents liquid circulation rate. Figure 7 depicts the plot of  $Nr$  at various impeller clearances at different radial positions.  $Nr$  slightly decreases from  $C/T = 0.33$  to 0.19 and drastically reduces at  $C^*$  where the flow transition was observed and becomes constant for further lower clearances. This change is observed because of velocity vector inclination, as radial pumping capacity is an integral function of radial velocity. It is found that the radial pumping capacity increases with increase in radial distance (Figure 7) due to fluid entrainment which match with literature data [9].

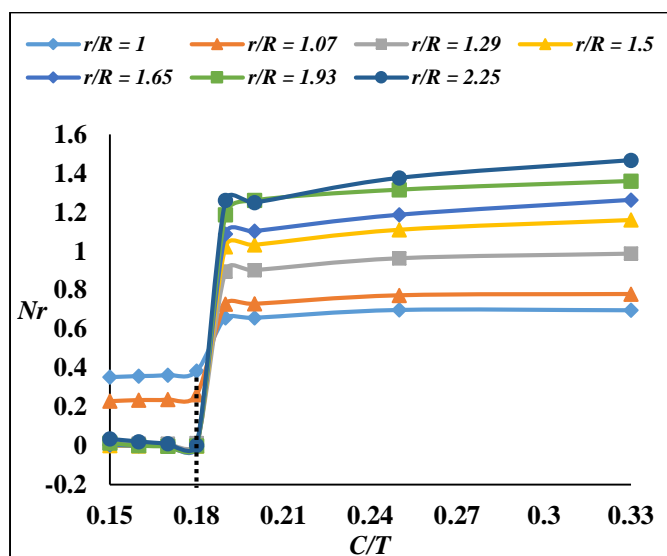


Figure 7: Dependence of radial pumping number on impeller clearance

#### 4.5 Effect of impeller clearance on Turbulent Kinetic Energy

Figure 8 depicts the effect of impeller clearance on normalized profiles of Turbulent Kinetic Energy (TKE). TKE decreases with lowering the impeller clearance and the value of peak is found to be reduced in considerable amount at  $C^*$ . Also, the location of peak has been shifted below the impeller centre plane and this is again due to of impeller discharge stream inclination.

#### 5 CONCLUSIONS

CFD simulations were conducted for Rushton turbine stirred tank. Double to single circulation loop flow transition observed at impeller clearance  $C^* = C/T = 0.18$ . At  $C^*$ , the power number was found to be decreased by 30% in comparison  $C/T = 0.33$  (standard). The radial velocity was decreased while axial velocity was increased with lowering impeller clearance. Radial pumping number sharply decreased at  $C^*$  and it increased with increase in radial distance. The turbulent kinetic energy also reduced with lowering the impeller clearance. Thus radial as well as turbulent action of Rushton turbine changes to axial nature as impeller clearance reduces below  $C^*$ .

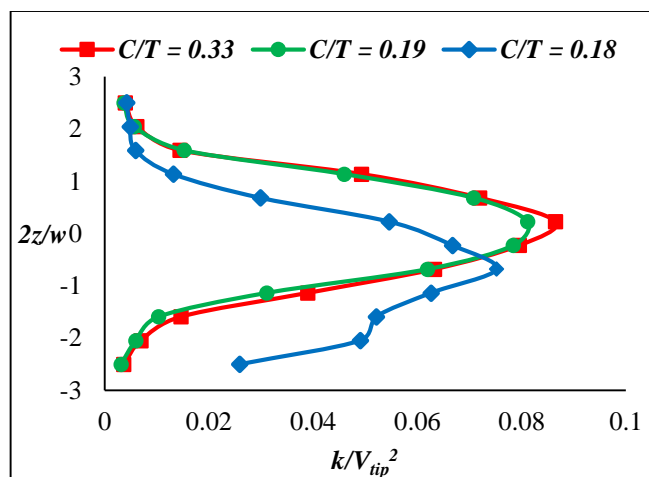


Figure 8: Axial profiles of normalized turbulent kinetic energy at  $r = 5.55$  cm and  $\theta = 45^\circ$

#### REFERENCES

- [1] N. K. Nere, A. W. Patwardhan, J. B. Joshi, (2003), Liquid phase mixing in stirred vessels turbulent flow regime, *Ind. Eng. Chem. Res.*, 42, 2661-2698.
- [2] V. Buwa, A. Dewan, A. F. Nassar, F. Durst, (2006), Fluid dynamics and mixing of single phase flow in a stirred vessel with a grid disc experimental and numerical investigations, *Chem. Engg. Sci.*, 61, 2815-2822.
- [3] A. W. Nienow, (1968), Suspensions of solid particles in turbine agitated baffled vessels, *Chem. Engg. Sci.*, 23, 1453-1459.
- [4] P. M. Armenante, E. U. Nagamine, (1998), Effect of low off bottom impeller clearance on minimum agitation speed for complete suspension of solids in stirred tanks, *Chem. Engg. Sci.*, 53(9), 1757-177.
- [5] G. Montante, K. C. Lee, A. Brucato, M. Yianneskis, (1999), An experimental study of double to single loop transition in stirred vessels, *The Can. J. Chem. Engg.*, 77, 649-659.
- [6] G. Montante, K. C. Lee, A. Brucato, M. Yianneskis, (2001), Numerical simulations of the dependency of flow pattern on impeller clearance in stirred vessels, *Chem. Engg. Sci.*, 56, 3751-3770.
- [7] ANSYS Inc., (2013). ANSYS Fluent 15 theory guide, Canonsburg, Pennsylvania.
- [8] H. Bashiri, E. Alizadeh, f. Bertrand, J. Chauki, (2016). Investigation of turbulent fluid flow in stirred tanks using a non-intrusive particle tracking technique. *Chem. Eng. Sci.* 140, 233-251.
- [9] H. Wu and G. Patterson, (1989), Laser Doppler measurements of turbulent flow parameters in a stirred mixer, *Chem. Eng. Sci.* 44, 2207-2221.